brains of patients with Alzheimer's disease[14–17]. In addition, active m-calpain accumulates in neurofibrillary tangles in Alzheimer's disease brains[14].

The amyloid hypothesis proposes that the Aβ peptides, perhaps acting with other influences such as excitotoxins, free radicals and oxidative stress, cause an increased or unregulated entry of calcium into affected cells, which ultimately leads to the activation of a tau-phosphorylating kinase[18]. Our observations indicate that cdk5 may be one of the kinases 'activated' by amyloid-β peptide through calpain-mediated conversion of p35 to p25 (Fig. 5d). Given the potentially deleterious role of cdk5 in Alzheimer's disease, the calpain-mediated p35 cleavage pathway may serve as a target for pharmacological intervention. □

Methods

Chemicals and antibodies

p25 antibody was raised against the whole protein and purified against glutathione *S*-transferase (GST)−p25. Non-erythroid α-spectrin antibody was purchased from Chemicon. p35 C-19, p35 N-20 and μ-calpain polyclonal antibodies were purchased from Santa-Cruz. The anti-rat m-calpain antibody is a gift from J. Elce. PMSF, Pepstatin A, aprotinin, leupeptin, MTT, glutamate and all metal chlorides were purchased from Sigma. Purified calpain I, purified calpain II, calpastatin, calpeptin, calpain inhibitor I, calpain inhibitor II, BAPTA-AM, butyrolactone and ionomycin were purchased from Calbiochem. H_2O_2 was purchased from Fisher Scientific. Aβ(1–42) and Aβ(42–1) were purchased from Bachem.

Primary cortical neuronal cultures

E17–E19 pregnant Long Evans rats were purchased from Harland Sprague–Dawley. Embryos were surgically removed and their cortices were dissected and cultured as described[3]. Cortical cultures were grown in basal growth medium on 6-well plates coated with laminin and poly-D-lysine. Treatments with H_2O_2 and glutamate were performed 10 d after plating for 5 h. Treatment with ionomycin was performed 4 d after plating for 5 h. In experiments where calpeptin, EGTA, or BAPTA-AM were used, the drugs were added 30 min before challenges were applied.

Glycerol gradient

A 11-ml 10–25% glycerol gradient was set up in ELB buffer (50 mM Tris pH 7, 0.1% NP-40, 250 mM NaCl). We layered 300 μl of fresh mouse brain lysate on top of the gradient and centrifuged at 40K r.p.m. for 26 h. We collected 17 600-μl fractions. We incubated 10 μl of each fraction at 25 °C for 2 h with either purified p35 or frozen and thawed mouse brain lysates in a reaction buffer (5 mM CaCl2, 5 mM cysteine, 150 mM imidazole, pH 7.5) to a final volume of 100 μl. The product from each reaction was electrophoresed on a 12% gel and analysed as described in the text.

Protein microsequencing

Recombinant p35 and His-tagged cdk5 were produced by baculovirus and the p35/cdk5 complex was purified through a Ni^{2+} column. We treated 1 μg of the purified p35/cdk5 complex with 2 units of purified m-calpain (Calbiochem) at 30 °C for 30 min. The reaction was stopped by 1% SDS. The entire reaction was electrophoresed on a 15% acrylamide gel and transferred to a 0.2-μm PVDF membrane (BioRad). The membrane was stained with Coomassie Brilliant Blue (BioRad), the 25K cleavage product was excised, and 1/3 of the excised band was sequenced on Applied Biosystems Model 494 Procise Protein Sequencer with Model 140C Microgradient Delivery System and Model 785A Programmable Absorbance Detector.

Ischaemia

To induce focal ischaemia, adult mice (C57BL/6), weighing 16–20 g, were anaesthetized initially with 1.5% isoflurane and thereafter maintained in 1.0% isoflurane in 70% N_2O and 30% O_2. An 8.0 nylon monofilament suture coated with a silicone/hardener mixture (Heraeus Kulzer) was inserted into the right common carotid artery. The suture was advanced 9–10 mm from the insertion site through the internal carotid artery, occluding the middle cerebral artery (MCA). Mice all woke up hemiplegic and were killed with isoflurane 4 h after the induction of ischaemia. Global ischaemia was induced for 1 h as described[19]. Generation and fractionation of brain lysates was as described[20].

Cell viability assay

Primary cortical neurons were plated on 96-well plates. Four days after plating, neurons were incubated with 20 μM Aβ(1–42) (from a stock of 1 mg ml^{-1} in ddH_2O) with or without 10 μM butyrolactone (from 2.8 mM stock in DMSO) or 20 μM calpeptin (from 2 mM stock in DMSO) for 24 h. Cell viability was measured by treating neurons with MTT (Sigma) at a final concentration of 0.5 mg ml^{-1} for 1 h. After MTT treatment, cell medium was replaced with 100 μl DMSO and the optical density of each well at 495 nm was determined using a microtitre plate reader.

Received 16 December 1999; accepted 7 April 2000.

1. Ohshima, T. *et al.* Targeted disruption of the cyclin-dependent kinase 5 gene results in abnormal corticogenesis, neuronal pathology and perinatal death. *Proc. Natl Acad. Sci. USA* **93,** 11173–11178 (1996).
2. Chae, T. *et al.* Mice lacking p35, a neuronal specific activator of Cdk5, display cortical lamination defects, seizures, and adult lethality. *Neuron* **18,** 29–42 (1997).
3. Nikolic, M., Dudek, H., Kwon, Y. T., Ramos, Y. F. & Tsai, L. H. The cdk5/p35 kinase is essential for neurite outgrowth during neuronal differentiation. *Genes Dev.* **10,** 816–825 (1996).
4. Patrick, G. N. *et al.* Conversion of p35 to p25 de-regulates cdk5 activity and promotes neurodegeneration. *Nature* **402,** 615–622 (1999).
5. Wang, K. K. W. in *Calpain: Pharmacology and Toxicology of Calcium-Dependent Protease* (eds Wang, K. K. W. & Yuen, P.-W.) 77–102 (Taylor & Francis, Philadelphia, 1999).
6. Sorimachi, H., Ishiura, S. & Suzuki, K. Structure and physiological function of calpains. *Biochem. J.* **328,** 721–732 (1997).
7. Lew, J. *et al.* A brain-specific activator of cyclin-dependent kinase 5. *Nature* **371**, 423–426 (1994).
8. Yankner, B. A. Mechanisms of neuronal degeneration in Alzheimer's disease. *Neuron* **16,** 921–932 (1996).
9. Alvarez, A., Toro, R., Caceres, A. & Maccioni, R. B. Inhibition of tau phosphorylating protein kinase cdk5 prevents β-amyloid-induced neuronal death. *FEBS Lett.* **459,** 421–426 (1999).
10. Arispe, N., Pollard, H. B. & Rojas, E. Giant multilevel cation channels formed by Alzheimer disease amyloid beta protein [A beta P-(1-40)] in bilayer membranes. *Proc. Natl Acad. Sci. USA* **90,** 10573–10577 (1993).
11. Hartmann, H., Eckert, A. & Muller, W. E. β-Amyloid protein amplifies calcium signalling in central neurons from the adult mouse. *Biochem. Biophys. Res. Commun.* **194,** 1216–1220 (1993).
12. Mattson, M. P. *et al.* β-Amyloid peptides destabilize calcium homeostasis and render human cortical neurons vulnerable to excitotoxicity. *J. Neurosci.* **12,** 376–389 (1992).
13. Pascale, A. & Etcheberrigaray, R. Calcium alterations in Alzheimer's disease: pathophysiology, models and therapeutic opportunities. *Pharmacol. Res.* **39,** 81–88 (1999).
14. Grynspan, R., Griffin, W. R., Cataldo, A., Katayama, S. & Nixon, R. A. Active site-directed antibodies identify calpain II as an early-appearing and pervasive component of neurofibrillary pathology in Alzheimer's disease. *Brain Res.* **763,** 145–158 (1997).
15. Nixon, R. A. *et al.* Calcium-activated neutral proteinase (calpain) system in aging and Alzheimer's disease. *Ann. NY Acad. Sci.* **747,** 77–91 (1994).
16. Saito, K., Elce, J. S., Hamos, J. E. & Nixon, R. A. Widespread activation of calcium-activated neutral proteinase (calpain) in the brain in Alzheimer disease: a potential molecular basis for neuronal degeneration. *Proc. Natl Acad. Sci. USA* **90,** 2628–2632 (1993).
17. Iwamoto, N., Thangnipon, W., Crawford, C. & Emson, P. C. Localization of calpain immunoreactivity in senile plaques and in neurones undergoing neurofibrillary degeneration in Alzheimer's disease. *Brain Res.* **561,** 177–180 (1991).
18. Selkoe, D. J. Translating cell biology into therapeutic advances in Alzheimer's disease. *Nature* **399,** A23–A31 (1999).
19. Seisjo, B. K. in *Brain Energy Metabolism* 454 (Wiley, New York, 1978).
20. Nikolic, M., Chou, M. M., Lu, W., Mayer, B. J. & Tsai, L. H. The p35/Cdk5 kinase is a neuron-specific Rac effector that inhibits Pak1 activity. *Nature* **395,** 194–198 (1998).

Acknowledgements

We thank J. Elce for the m-calpain antibody; A. Bonni and V. Tannoch for reading this manuscript; M. Ahlijanian, B. Yankner, E. Wang, K. Kosik and members of the Tsai lab for discussions. This work was partially supported by NIH grants to L.-H.T. L.-H.T. is an assistant investigator of the Howard Hughes Medical Institute, a Rita Allen Foundation scholar and a recipient of an Ester A. and Joseph Kligenstein Fund grant.

Correspondence and requests for materials should be addressed to L.-H.T. (e-mail: li-huei_tsai@hms.harvard.edu).

Supplementary information is available from *Nature*'s World-Wide Web site (http://www.nature.com) or as paper copy from the London editorial office of *Nature*.

LAG-3 is a putative transcriptional activator in the *C. elegans* Notch pathway

Andrei G. Petcherski & Judith Kimble

Howard Hughes Medical Institute and Department of Biochemistry, University of Wisconsin-Madison, 433 Babcock Drive, Madison, Wisconsin 53706, USA

Notch signalling controls growth, differentiation and patterning during normal animal development[1,2]; in humans, aberrant Notch signalling has been implicated in cancer and stroke[3,4]. The mechanism of Notch signalling is thought to require cleavage of the receptor in response to ligand binding[5], movement of the receptor's intracellular domain to the nucleus[6,7], and binding of that intracellular domain to a CSL (for CBF1, Suppressor of

Hairless, LAG-1)[8,9] protein. Here we identify LAG-3, a glutamine-rich protein that forms a ternary complex together with the LAG-1 DNA-binding protein[10] and the receptor's intracellular domain. Receptors with mutant ankyrin repeats that abrogate signal transduction are incapable of complex formation both in yeast and *in vitro*. Using RNA interference, we find that LAG-3 activity is crucial in *Caenorhabditis elegans* for both GLP-1 and LIN-12 signalling. LAG-3 is a potent transcriptional activator in yeast, and a Myc-tagged LAG-3 is predominantly nuclear in *C. elegans*. We propose that GLP-1 and LIN-12 promote signalling by recruiting LAG-3 to target promoters, where it functions as a transcriptional activator.

The *C. elegans* Notch signalling pathway relies on either of two receptors, GLP-1 or LIN-12 (Fig. 1a)[1,2]. The intracellular portions of GLP-1 and LIN-12 possess three distinct regions: the RAM domain binds tightly and specifically to LAG-1 (ref. 8); the ankyrin repeats (ANK) are critical for signalling[11–13]; and the PEST domain is thought to control receptor stability[14] (Fig. 1b). Among these domains, the RAM and ANK regions are sufficient for eliciting a strong signalling response[8].

We used a modified yeast two-hybrid screen to identify proteins that interact with the GLP-1 intracellular domain only in the presence of LAG-1. Briefly, one hybrid protein, GLP-1(RAM-ANK), fused to the LexA DNA-binding domain and one non-hybrid protein, LAG-1, were used as a complex bait, selecting for activation of the *HIS3* gene in the presence of a *C. elegans* complementary DNA/activation domain fusion library (see Methods). Out of 300,000 transformants, 6 were dependent on the presence of LAG-1 for robust growth; all 6 positives carried a complementary DNA encoding the same glutamine-rich protein (Fig. 1c), which we call LAG-3. In yeast, LAG-3 interacts strongly with both GLP-1(RAM-ANK) and LIN-12(RAM-ANK) in the presence of LAG-1, but not in its absence (Fig. 1d). Furthermore, LAG-3 does not interact with either LAG-1 alone or a lamin control (Fig. 1d). The simplest interpretation is that a ternary complex is formed which is composed of LAG-3, LAG-1 and either GLP-1(RAM-ANK) or LIN-12(RAM-ANK).

We then assayed formation of the complex *in vitro*. We generated a LAG-1 carrying a T7 epitope tag (Novagen) bound to beads and versions of the remaining components, each bearing an S-peptide tag (Novagen). After incubation, the proteins associating with beads were detected by western blot (see Methods). LAG-3 bound LAG-1 in the presence of wild-type GLP-1(RAM-ANK) (Fig. 2a, lane 3), but did not bind LAG-1 alone (Fig. 2a, lane 7). As expected from previous results[8], GLP-1(RAM-ANK) bound LAG-1 regardless of LAG-3 (Fig. 2a, lane 5). To determine whether LAG-3 binds GLP-1(RAM-ANK) on its own, we carried out a reciprocal experiment with T7–LAG-3 bound to beads and S-tagged versions of LAG-1 and GLP-1(RAM-ANK). Wild-type GLP-1(RAM-ANK) bound weakly to LAG-3 (Fig. 2b, lanes 7, 8), but binding was enhanced markedly by the addition of LAG-1 (Fig. 2b, lanes 3, 4). We conclude that a ternary complex composed of LAG-1, LAG-3 and the RAM-ANK region of GLP-1 forms *in vitro*.

Previous work has shown that the ANK repeats of both GLP-1 and LIN-12 are essential for signalling[11–13]. To determine whether ANK repeat mutations disrupted ternary complex formation, we assayed three mutations in the fourth ANK repeat of either GLP-1 or

Table 1 Wild-type ANK repeats are required in yeast for complex formation and LAG-3 is a potent transcriptional activator in yeast

AD–Lag-3	T (°C)	GLP-1(RAM-ANK)*			LIN-12(RAM-ANK)*		LAG-1*	Lamin*
		wt	*q224*	*q231*	wt	*n653*		
Lag-1	15	++++	++++	++++	++++	–	±	–
	20	++++	++	++++	++++	–	–	–
	25	++++	+	+++	+++	–	–	–
	30	++++	+	++	++	–	–	–
no Lag-1	15	++	–	–	–	–	±	–
	20	++	–	–	–	–	–	–
	25	++	–	–	–	–	–	–
	30	++	–	–	–	–	±	–

	GLP-1(RAM-ANK)*			LIN-12(RAM-ANK)*		LAG-1*	LAG-3*	Lamin*
	wt	*q224*	*q231*	wt	*n653*			
	±	–	–	–	–	±	++++	–

*LexA fusion proteins were used. T, temperature of yeast growth. Scale for β-galactosidase activity: ++++, strong blue colour detected by 30 min; +++, by 60 min; ++, by 90 min; +, by 120 min; ±, by 4 h; –, no blue detected at 4 h.

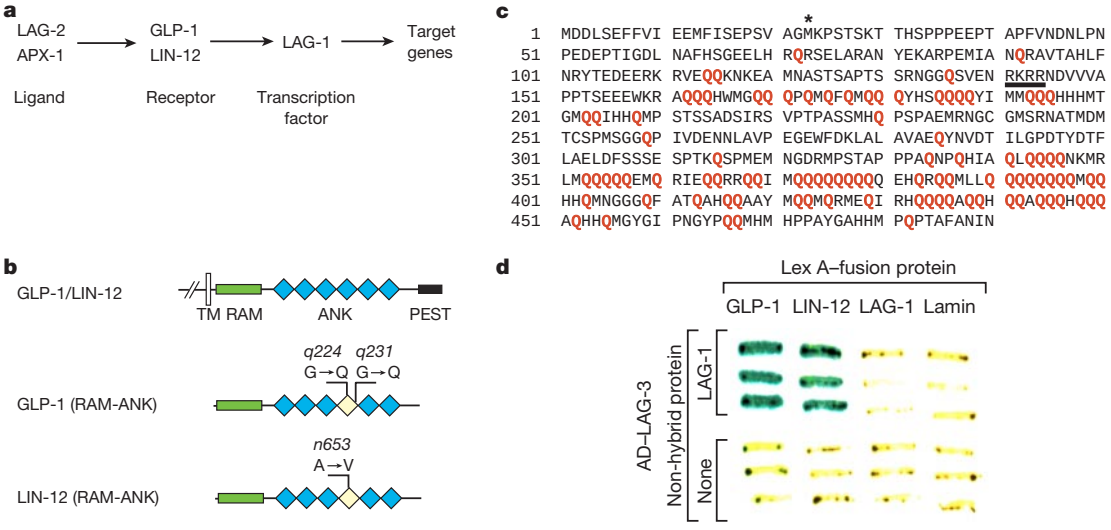

Figure 1 LAG-3 and ternary complex formation in yeast. **a**, Core components of the GLP-1/LIN-12 pathway (reviewed in ref. 1). **b**, Intracellular domain of receptors. Top, wild type proteins. TM, transmembrane domain; RAM, RAM domain (green box); ANK, ankyrin repeats (blue diamonds); PEST, PEST domain (black box). Middle, GLP-1 mutant protein. Bottom, LIN-12 mutant protein. **c**, LAG-3 amino-acid sequence. Glutamine is highlighted in red; the predicted nuclear localization sequence is underlined. Two alternative 5′ ends predict two proteins, LAG-3A and LAG-3B (see Methods). Asterisk denotes the methionine predicted to initiate LAG-3B. **d**, Interactions of LAG-1, LAG-3 and GLP-1(RAM-ANK) or LIN-12(RAM-ANK) proteins in yeast. Transcription by LexA-controlled reporter yields β-galactosidase (blue). Top, LexA fusion proteins; side, AD–LAG-3, GAL-4-activation domain fused to LAG-3. Yeast were grown at 20 °C.

LIN-12 (Fig. 1b); all three mutant proteins were produced stably in yeast as shown by western blot (not shown). In *C. elegans,* the *glp-1(q224)* and *glp-1(q231)* mutant receptors signal almost normally at 15 °C, but function poorly at 20 °C and 25 °C (ref. 15). When assayed in yeast, both mutants were defective for ternary complex formation in a temperature-sensitive manner: interactions were indistinguishable from wild-type at 15 °C, but much weaker at 30 °C (Table 1). Moreover, the strength of interaction correlated with allelic strength: the weaker *q231* mutant interacted better in yeast than did the more severe *q224* mutant. Similarly for *lin-12*, the *lin-12(n653)* mutant receptor is severely impaired in *C. elegans*[12], and when assayed in yeast, LIN-12(RAM-ANKn653) did not participate in complex formation (Table 1). Finally, when the mutant GLP-1(RAM-ANKq224) protein was assayed *in vitro,* formation of the ternary complex was not detectable (Fig. 2a, lane 4; Fig. 2b, lanes 5, 6). We conclude that the ANK repeats of both GLP-1 and LIN-12 receptors are critical for interactions with LAG-1 and LAG-3, and suggest that the failure of the mutant receptors to function properly in *C. elegans* may be due to their inability to form ternary complexes.

We then determined whether *lag-3* activity is required for *glp-1* and *lin-12* signalling in *C. elegans*. We used RNA interference (RNAi)[16] to reduce *lag-3* activity (see Methods). To examine the effects of *lag-3(RNAi)* on early embryos, mothers were soaked in double-stranded (ds) *lag-3* RNA as late L4 larvae. Whereas wild-type embryos have an elongate pharynx (Fig. 3a), both *glp-1(q224)* and *lag-3(RNAi)* embryos lack an anterior pharynx and die within the eggshell (Fig. 3b, c). To examine the effects of *lag-3(RNAi)* postembryonically, early L1 larvae were soaked in *lag-3* dsRNA. Resultant *lag-3(RNAi)* adults were usually sterile (91%, $n = 100$), and sometimes possessed a protruding vulva (36%, $n = 100$). The sterility of *lag-3(RNAi)* adults resulted from a failure in germline proliferation (Fig. 3d, e), a phenotype typical of *glp-1* null mutants[15]; the protruding vulva (Fig. 3f) was similar to that of *lin-12* loss-of-function mutants[17]. More diagnostic of a *lin-12* signalling defect, however, was the finding of two anchor cells in *lag-3(RNAi)* larvae (Fig. 3g). Also, these *lin-12* and *glp-1* defects were the only ones observed and, therefore, other pathways appear to be unaffected. From these results, we conclude that *lag-3* is critical for *glp-1* signalling in both embryo and germ line and for *lin-12* signalling postembryonically.

To further investigate the role of *lag-3* in *C. elegans*, we assayed the effect of *lag-3(RNAi)* on both *glp-1* and *lin-12* gain-of-function mutants. Whereas most *glp-1(oz112 gf)* animals are sterile and make tumorous germ lines at 25 °C (ref. 18) (Fig. 3h, upper row), most *glp-1(oz112 gf); lag-3(RNAi)* adults are either fertile or sterile with a Glp-1-like germ line composed solely of a few mature sperm (Fig. 3h, lower row). Thus, *lag-3* is critical for *glp-1(gf)* signalling. Similarly for *lin-12,* all *lin-12(n137 gf)* mutants possess multiple pseudovulvae, the Muv phenotype (Fig. 3i, upper row), and do not possess an anchor cell[17], whereas most *lin-12(n137 gf); lag-3(RNAi)* animals have either a normal or a Lin-12-like protruding vulva (Fig. 3i, lower row). Upon examination by DIC microscopy, most

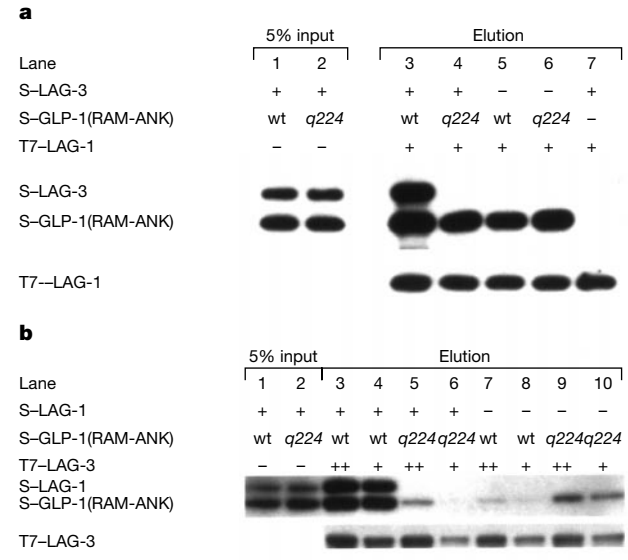

Figure 2 LAG-3 forms a ternary complex *in vitro* with GLP-1(RAM-ANK) and LAG-1. **a**, LAG-3 binds LAG-1 in the presence of wild-type GLP-1(RAM-ANK). Lanes 1, 2, input S-tagged proteins; lane 3–10, T7–LAG-1 was bound to beads; proteins incubated with beads shown at top of each lane. **b**, LAG-1 binds LAG-3 in presence of wild-type GLP-1. Lanes 1, 2, input S-tagged proteins; lanes 3–10, T7–LAG-3 was bound to beads; proteins incubated with beads shown at top of each lane. Assays done in duplicate using two different amounts of LAG-3 for each experiment (++ indicates that the amount of T7–LAG-3 is ~3 times greater than +).

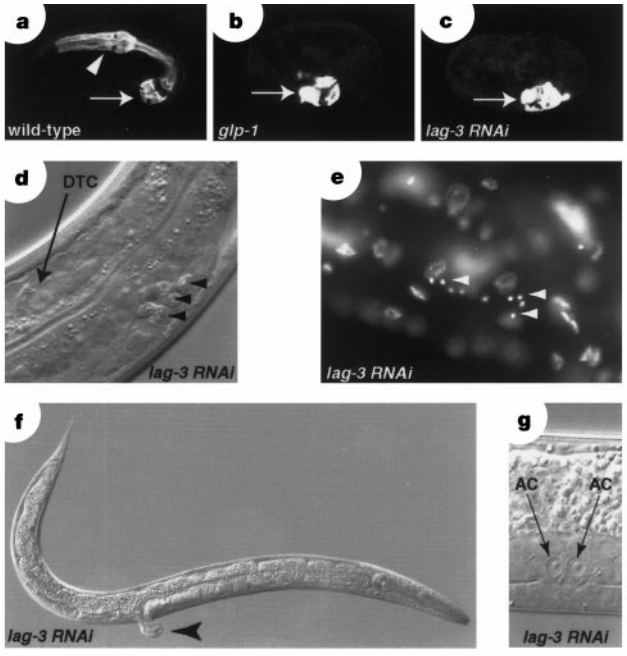

h

genotype	RNAi	PHENOTYPE Glp	Fertile	Tumorous	Exploded	*n*
glp-1 (gf)	Buffer	0%	0%	96%	4%	46
glp-1 (gf)	*lag-3*	30%	30%	28%	11%	53

i

genotype	RNAi	PHENOTYPE Protruding vulva	Normal vulva	Others	Muv	Average number of vulvae
lin-12 (gf)	Buffer	0% (*n*=20)	0% (*n*=20)	0% (*n*=20)	100% (*n*=20)	4.95 (*n*=20)
lin-12 (gf)	*lag-3*	57% (*n*=70)	11% (*n*=70)	32% (*n*=70)	0% (*n*=41)	1.37 (*n*=41)

Figure 3 *lag-3* is critical for both *glp-1* and *lin-12* signalling. **a**–**c**, Embryos stained with 3NB12 antibody: arrowhead, anterior pharynx; arrow, posterior pharynx. **d**–**e**, *lag-3(RNAi)* adults with germ line composed solely of a few mature sperm (arrowheads). **d**, Distal tip cell (DTC). **e**, 4′,6-diamidino-2-phenylindole (DAPI) stained. **f**, *lag-3(RNAi)* adult with protruding vulva (arrowhead). **g**, *lag-3(RNAi)* L3 with two anchor cells (AC) (arrows). **h**–**i**, Suppression of *glp-1(oz112 gf)* and *lin-12(n137 gf)* by *lag-3(RNAi)*. L1s soaked with either *lag-3* dsRNA or M9 buffer. *n*, number of animals. **h**, Complete genotype: *unc-32(e189) glp-1(oz112 gf)*. Glp, *glp-1(lf)* phenotype. Tumorous, *glp-1(gf)* phenotype. Exploded indicates that animals could not be scored. **i**, Suppression of *lin-12(n137 gf)* by *lag-3(RNAi)*. Protruding vulva, *lin-12(lf)* phenotype; others, minor vulval defects. Muv, *lin-12(gf)* phenotype.

lin-12(gf); lag-3(RNAi) animals possessed at least one anchor cell (data not shown). Both *glp-1(gf)* and *lin-12(gf)* receptors therefore rely on *lag-3* activity for signalling. We conclude that *lag-3* is an integral component of both *glp-1* and *lin-12* signalling pathways.

How might LAG-3 function in signal transduction? The LAG-3 amino-acid sequence is glutamine-rich, containing 20% glutamine residues (Fig. 1c), a hallmark of certain transcriptional activation domains[19]. To determine whether LAG-3 might function in transcriptional control, we did two experiments. First, we tested a LexA–LAG-3 fusion protein for its ability to activate transcription in yeast, and found it to be a strong transcriptional activator (Table 1). In contrast, other nuclear components of the *glp-1/lin-12* pathway possessed either no activity by this assay or a much more modest activity (Table 1). Second, we examined the subcellular localization of a Myc-tagged LAG-3 fusion protein placed under heat shock control and introduced into transgenic animals. Upon heat shock, Myc–LAG-3 was predominantly nuclear (Fig. 4a), whereas without heat shock, virtually no staining could be detected (Fig. 4b). Consistent with the idea that LAG-3 is a nuclear protein, there is a classical nuclear localization signal[20] in its amino-acid sequence (Fig. 1c, underline). The simplest interpretation is that LAG-3 normally serves as a transcriptional activator and that the primary function of the receptor's intracellular domain is to bring LAG-3 and LAG-1 together in a ternary complex at the target gene promoter.

Figure 4c,d illustrates one model of how LAG-3 and ternary complex formation might function in *glp-1* and *lin-12* signalling. In the absence of ligand binding (Fig. 4c), the receptor's intracellular domain does not enter the nucleus and LAG-3 is not recruited to target gene promoters. Upon ligand binding (Fig. 4d), however, the receptor is cleaved and its intracellular domain moves to the nucleus; as a result, LAG-3 is recruited to the promoter as part of a ternary complex, activating transcription. It must be emphasized that this model is speculative. For example, both the specific binding interactions within the ternary complex and the stoichiometry of components within the complex are not known. If LAG-3 is indeed a transcriptional activator in *C. elegans,* which we think is likely, the LAG-3 glutamine-rich domain might serve as the primary activation domain, as illustrated, or it might act together with other proteins, for example with the receptor's intracellular domain.

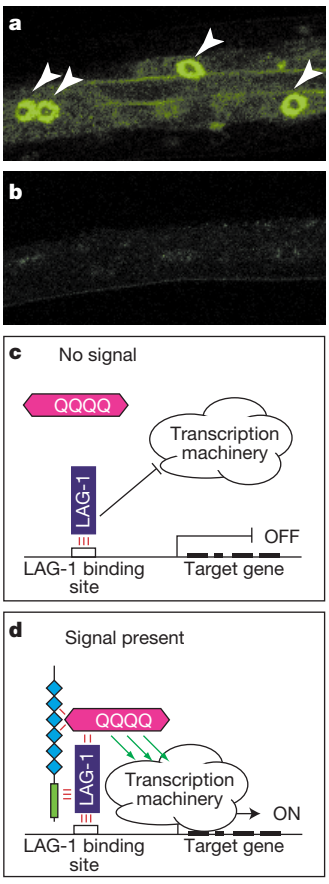

Figure 4 LAG-3 may function as a transcriptional activator. **a**,**b**, Adults carrying Myc–LAG-3 under heat shock control, examined using anti-Myc antibodies. **a**, After heat shock, Myc-LAG-3 is predominantly nuclear, as seen in intestinal nuclei (arrowheads). **b**, Without heat shock, Myc-LAG-3 is barely detectable. **c**,**d**, Model for LAG-3 function. **c**, Without signalling, no ternary complex is formed at target gene promoter and transcription is repressed. **d**, Upon signalling, the ternary complex forms and transcription is activated.

The identification of a new component in the *C. elegans glp-1/lin-12* signalling pathway has important implications for our understanding of Notch signalling. In particular, evidence suggests that a *lag-3*-like activity will be found in *Drosophila* and vertebrates. First, the strong conservation among CSL DNA-binding proteins and the conservation of both RAM and ANK repeat regions in all Notch-like receptors suggests that these proteins participate in a conserved process. Second, missense mutations in the ANK repeats of *Drosophila* Notch[21] and mouse Notch1 (ref. 22) reduce the ability of receptor activity to induce cell fate changes, as also found in *C. elegans*. Last, mouse Notch1 ANK mutants fail to induce target gene transcription[23,24]. As the *C. elegans* ANK mutations abrogate ternary complex formation, we predict that ANK mutations in other Notch-related receptors similarly affect complex formation with a LAG-3-like protein and the CSL DNA-binding protein. That LAG-3 activity might be provided by a component of the Notch pathway, such as *mastermind*[25], which so far has not found a place in models for molecular mechanism, or some other protein that has yet to be identified. Identification of the third partner and analysis of the ternary complex will be essential for understanding how normal Notch signalling controls development and physiology and how aberrant Notch signalling leads to human disease.

Note added in proof: *lag-3* has also been shown to correspond to the previously described locus *sel-8* and to be associated with Lag phenotypes in RNAi experiments (T. Doyle and I. Greenwald, personal communication). □

Methods

Yeast two-hybrid screen and assays

The yeast two-hybrid screen was done essentially as described[26] with two modifications. First, we used the L40-*ura3* (*MATa, trp1, his3, leu2, ade2, LYS2::(LexAop)4-HIS3, ura3::(LexAop)8-lacZ*) yeast strain (a gift from T. Triolo and R. Sternglanz) for both screening and characterization of interactions. Second, in addition to LexA and AD fusion proteins, a third, 'non-hybrid' protein, LAG-1, was expressed from pYES2 vector (Invitrogen). The screen used the plasmid form of a *C. elegans* cDNA library fused to Gal4-AD, which was derived from the LambdaACT-pRB-2 library[27]. Among the six *lag-3* cDNAs recovered, three were full-length for LAG-3A (residues 1–490) and the others encoded truncated forms (residues 1–398, 1–446 and 24–490). The β-galactosidase filter-lift assay was done as described[26]. For assays of yeast grown at different temperatures, yeast were grown on plates at the given temperature, frozen in liquid nitrogen and the enzymatic assay carried out at 30 °C.

Plasmids

Plasmids were constructed using standard techniques and details are available upon request. The pBTM116 vector[26] was used to obtain LexA fusions. All LexA–GLP-1(RAM-ANK) constructs encode GLP-1 residues 788–1171; mutant versions contain appropriate nucleotide substitutions[13]. LexA–LIN-12(RAM-ANK) constructs encode LIN-12 residues 930–1320, the mutant version contains the appropriate nucleotide substitution[12]. LexA–LAG-3 encodes residues 1–490 of LAG-3. The LexA–Lamin fusion has been described[26]. The non-hybrid used for the yeast two-hybrid screen contained residues 203–673 of LAG-1. AD–LAG-3 contains residues 1–490 of LAG-3A. pCITE-4a (Novagen) was used to obtain S-tag fusion proteins,. S–LAG-1 includes residues 199–673 of LAG-1. S–GLP-1(RAM-ANK), wild type and mutant, encodes residues 788–1171 of GLP-1. S–LAG-3 encodes residues 5-490 of LAG-3A. pET-28a (Novagen) was used to generate T7-tag fusions. T7–LAG-1 encodes residues 199–673 of LAG-1; T7–LAG-3 encodes residues 5–490 of LAG-3. For LAG-3 localization in worms, a Myc–LAG-3 construct, encoding full-length LAG-3A, was created from a modified pPD49.83, which contains the heat shock promoter HSP16-14, a translation start site, and an amino-terminal c-Myc epitope[8].

In vitro binding assay

T7-tagged proteins were produced in *Escherichia coli* and partially purified by absorption onto T7-tag antibody agarose. S-tagged proteins were generated using rabbit reticulocite lysate (TnT, Promega). *In vitro* translated proteins were diluted with 0.5 ml of T7-tag bind/wash buffer (4.29 mM Na_2HPO_4, 1.47 mM KH_2PO_4, 2.7 mM KCl, 137 mM NaCl, 0.1% Tween-20, 0.002% NaN_3, pH 7.3) in the presence of 1 × 'Complete EDTA-free' protease inhibitor cocktail (Boehringer Mannheim). S-tagged proteins were then added to the corresponding T7-tagged protein bound to the agarose beads in microfuge tubes. Samples were incubated with shaking for 1 h at 25 °C. The agarose beads were washed three times with 1 ml of T7-tag bind/wash buffer in the presence of 1 × Complete EDTA-free protease inhibitor cocktail. Bound proteins were released by boiling agarose beads in protein loading buffer. Proteins were separated using SDS–PAGE and transferred to polyvinylidene difluoride membrane. S-tagged proteins were visualized using S-protein-alkaline phosphatase conjugates (Novagen); T7-tagged proteins were visualized using T7-tag antibody-alkaline phosphatase conjugates (Novagen). Between 0.5 μg and 5 μg of T7–LAG-1 or T7–LAG-3 and about 100 ng of each of the S-tagged proteins were used in each assay.

Transcript analysis

The 5′ end of the *lag-3* message was determined by RT–PCR using *lag-3* specific primers and a primer to the *trans*-splicing leader SL1. Two alternative 5′ ends were obtained. The inferred transcripts are predicted to encode two proteins, LAG-3A and LAG-3B.

RNA interference

The RNAi effect should be limited to *lag-3* specifically, because this gene is unique in the *C. elegans* genome[28]. The DNA template for *in vitro* transcription contained all of the coding sequence for LAG-3A and 86 nucleotides of the *lag-3* 3′ untranslated region. To assay the postembryonic *lag-3* phenotype, L1 larvae were soaked in 1–3 μg μl^{-1} of double stranded *lag-3* RNA for 48 h at 20 °C or 25 °C in M9 buffer (22 mM KH_2PO_4, 42 mM NaH_2PO_4, 85 mM NaCl, 1 mM $MgSO_4$) in the presence of *E. coli* (Absorbance 600 nm, 0.75–1.0). After soaking, animals were transferred to Petri dishes to continue development. To assay the embryonic *lag-3* phenotype, L4 animals were soaked in M9 containing 1 μg μl^{-1} *lag-3* dsRNA overnight, then transferred to plates to lay eggs, using essentially a described method[29].

Subcellular localization

Generation of transgenic nematodes carrying HS–Myc–LAG-3, heat shock conditions and antibody detection was done essentially as described[8], except a whole mount freeze cracking method was used for fixation of the worms[30].

Received 25 January; accepted 3 March 2000.

1. Kimble, J. & Simpson, P. The LIN-12/Notch signalling pathway and its regulation. *Annu. Rev. Cell Dev. Biol.* **13,** 333–361 (1997).
2. Artavanis-Tsakonas, S., Rand, M. D. & Lake, R. J. Notch signalling: cell fate control and signal integration in development. *Science* **284,** 770–776 (1999).
3. Ellisen, L. W. *et al.* TAN-1, the human homolog of the *Drosophila Notch* gene, is broken by chromosomal translocations in T lymphoblastic neoplasms. *Cell* **66,** 649–661 (1991).
4. Joutel, A. *et al.* Notch3 mutations in CADASIL, a hereditary adult-onset condition causing stroke and dementia. *Nature* **383,** 707–710 (1996).
5. Schroeter, E. H., Kisslinger, J. A. & Kopan, R. Notch1 signalling requires ligand-induced proteolytic release of intracellular domain. *Nature* **393,** 382–386 (1998).
6. Struhl, G. & Adachi, A. Nuclear access and action of Notch *in vivo*. *Cell* **93,** 649–660 (1998).
7. Lecourtois, M. & Schweisguth, F. Indirect evidence for Delta-dependent intracellular processing of notch in *Drosophila* embryos. *Curr. Biol.* **8,** 771–774 (1998).
8. Roehl, H., Bosenberg, M., Blelloch, R. & Kimble, J. Roles of the RAM and ANK domains in signalling by the *C. elegans* GLP-1 receptor. *EMBO J.* **15,** 7002–7012 (1996).
9. Tamura, K. *et al.* Physical interaction between a novel domain of receptor Notch and the transcription factor RBP-Jκ/Su(H). *Curr. Biol.* **5,** 1416–1423 (1995).
10. Christensen, S., Kodoyianni, V., Bosenberg, M., Friedman, L. & Kimble, J. *lag-1*, a gene required for *lin-12* and *glp-1* signalling in *Caenorhabditis elegans*, is homologous to human CBF1 and *Drosophila* Su(H). *Development* **122,** 1373–1383 (1996).
11. Roehl, H. & Kimble, J. Control of cell fate in *C. elegans* by a GLP-1 peptide consisting primarily of ankyrin repeats. *Nature* **364,** 632–635 (1993).
12. Greenwald, I. & Seydoux, G. Analysis of gain-of-function mutations of the *lin-12* gene of *Caenorhabditis elegans*. *Nature* **346,** 197–199 (1990).
13. Kodoyianni, V., Maine, E. M. & Kimble, J. Molecular basis of loss-of-function mutations in the *glp-1* gene of *Caenorhabditis elegans*. *Mol. Biol. Cell* **3,** 1199–1213 (1992).
14. Mango, S. E., Maine, E. M. & Kimble, J. Carboxy-terminal truncation activates *glp-1* protein to specify vulval fates in *Caenorhabditis elegans*. *Nature* **352,** 811–815 (1991).
15. Austin, J. & Kimble, J. *glp-1* is required in the germ line for regulation of the decision between mitosis and meiosis in *C. elegans*. *Cell* **51,** 589–599 (1987).
16. Fire, A. *et al.* Potent and specific genetic interference by double-stranded RNA in *Caenorhabditis elegans*. *Nature* **391,** 806–811 (1998).
17. Greenwald, I. S., Sternberg, P. W. & Horvitz, H. R. The *lin-12* locus specifies cell fates in *Caenorhabditis elegans*. *Cell* **34,** 435–444 (1983).
18. Berry, L. W., Westlund, B. & Schedl, T. Germ-line tumor formation caused by activation of *glp-1*, a *Caenorhabditis elegans* member of the *Notch* family of receptors. *Development* **124,** 925–936 (1997).
19. Mitchell, P. J. & Tjian, R. Transcriptional regulation in mammalian cells by sequence-specific DNA binding proteins. *Science* **245,** 371–378 (1989).
20. Hicks, G. R. & Raikhel, N. Y. Protein import into the nucleus: an integrated view. *Annu. Rev. Cell Dev. Biol.* **11,** 155–188 (1995).
21. Diederich, R. J., Matsuno, K., Hing, H. & Artavanis-Tsakonas, S. Cytosolic interaction between deltex and Notch ankyrin repeats implicates deltex in the Notch signalling pathway. *Development* **120,** 473–481 (1994).
22. Kopan, R., Nye, J. S. & Weintraub, H. The intracellular domain of mouse Notch: a constitutively activated repressor of myogenesis directed at the basic helix-loop-helix region of MyoD. *Development* **120,** 2385–2396 (1994).
23. Jarriault, S. *et al.* Signalling downstream of activated mammalian Notch. *Nature* **377,** 355–358 (1995).
24. Kato, H. *et al.* Involvement of RBP-J in biological functions of mouse Notch1 and its derivatives. *Development* **124,** 4133–4141 (1997).
25. Smoller, D. *et al.* The *Drosophila* neurogenic locus *mastermind* encodes a nuclear protein unusually rich in amino acid homopolymers. *Genes Dev.* **4,** 1688–1700 (1990).
26. Bartel, P. L. & Fields, S. (eds) *The Yeast Two-Hybrid System* (Oxford Univ. Press, New York, 1997).
27. Kraemer, B. *et al.* NANOS-3 and FBF proteins physically interact to control the sperm-oocyte switch in *Caenorhabditis elegans*. *Curr. Biol.* **9,** 1009–1018 (1999).
28. The *C. elegans* Sequencing Consortium. Genome sequence of the nematode *C. elegans*: a platform for investigating biology. *Science* **282,** 2012–2018 (1998); erratum *ibid* **283,** 35 (1999); erratum *ibid* **283,** 2103 (1998).
29. Subramaniam, K. & Seydoux, G. *nos-1* and *nos-2*, two genes related to *Drosophila nanos*, regulate primordial germ cell development and survival in *Caenorhabditis elegans*. *Development* **126,** 4861–4871 (1999).
30. Crittenden, S. L. & Kimble, J. in *Cell: A Laboratory Manual* (eds Spector, D., Goldman, R. & Leinwand, L.) 108.101–108.109 (Cold Spring Harbor Laboratory Press, Cold Spring Harbor, 1998).

Acknowledgements

We acknowledge A. Puoti for providing the plasmid form of the cDNA library; R. Sternglanz, S. M. Hollenberg and A. Grimson for yeast strains and plasmids; and A. Steinberg and L. Vanderploeg for help with the illustrations. A.G.P. is an Howard Hughes Medical Institute predoctoral fellow. J.K. is an investigator of the Howard Hughes Medical Institute.

Correspondence and requests for materials should be addressed to J.K. (e-mail: jekimble@facstaff.wisc.edu). The mRNA sequences for *lag-3A* and *lag-3B* have been deposited in GenBank under accession codes AF241846 and AF241847, respectively.

Translocation step size and mechanism of the RecBC DNA helicase

Piero R. Bianco & Stephen C. Kowalczykowski

Sections of Microbiology and of Molecular and Cellular Biology, University of California at Davis, Davis, California 95616, USA

DNA helicases are ubiquitous enzymes that unwind double-stranded DNA[1–3]. They are a diverse group of proteins that move in a linear fashion along a one-dimensional polymer lattice—DNA—by using a mechanism that couples nucleoside triphosphate hydrolysis to both translocation and double-stranded DNA unwinding to produce separate strands of DNA. The RecBC enzyme is a processive DNA helicase that functions in homologous recombination in *Escherichia coli*; it unwinds up to 6,250 base pairs per binding event and hydrolyses slightly more than one ATP molecule per base pair unwound. Here we show, by using a series of gapped oligonucleotide substrates, that this enzyme translocates along only one strand of duplex DNA in the 3′ → 5′ direction. The translocating enzyme will traverse, or 'step' across, single-stranded DNA gaps in defined steps that are 23 (±2) nucleotides in length. This step is much larger than the amount of double-stranded DNA that can be unwound using the free energy derived from hydrolysis of one molecule of ATP, implying that translocation and DNA unwinding are separate events. We propose that the RecBC enzyme both translocates and unwinds by a quantized, two-step, inchworm-like mechanism that may have parallels for translocation by other linear motor proteins.

DNA unwinding by RecBC enzyme initiates only at blunt or nearly blunt double-stranded DNA (dsDNA) ends; thus, it had not been possible to determine on which strand of DNA translocation occurs, or whether both DNA strands are required. We therefore